molecular pharmaceutics

ARTICLE

pubs.acs.org/molecularpharmaceutics

Effect of Octreotide−Polyethylene Glycol(100) Monostearate Modification on the Pharmacokinetics and Cellular Uptake of Nanostructured Lipid Carrier Loaded with Hydroxycamptothecine

Zhigui Su, Jiangxiu Niu, Yanyu Xiao, Qineng Ping,* Minjie Sun, Aiwen Huang, Weiliang You, Xiaoye Sang, and Dongfen Yuan

State Key Laboratory of Natural Medicines, China Pharmaceutical University, Nanjing-210009, PR China

Supporting Information

ABSTRACT: A new conjugate, octreotide−polyethylene glycol(100) monostearate (OPMS), was developed for the enhancement of targeting delivery of hydroxycamptothecine (HCPT) loaded in nanostructured lipid carrier (NLC). 2×10^{-3} and 5×10^{-3} mmol of OPMS were respectively used to modify NLC so that the targeted nanocarriers with low and high ligand density were obtained. For comparison, the pegylated NLCs without octreotide were prepared by adding equal molar amounts of polyethylene glycol(100) monostearate (PGMS). The relation between the modification levels and properties of various NLCs were studied in vivo and in vitro. At a high modification level, a slower release rate of HCPT and the more stable nanocarriers was achieved. At the same time, the fixed aqueous layer thickness (FALT) and average surface density of PEG chains (SD_{PEG}) was increased, but the distance (D) between two neighboring PEG grafting sites became narrower. The in vivo pharmacokinetic study in healthy rat indicated that the modified NLCs had a longer circulation than NLC ($P < 0.05$) due to pegylation effect and OPMS modified NLCs had larger MRT and AUC_{0-t} than that of PGMS modified NLCs at the same modification level. Furthermore, the florescence microscopy observation also showed the targeting effect of octreotide modification on somatostatin receptors (SSTRs) of tumor cell (SMMC-7721). The uptake of SMMC-7721 was much more than that of normal liver cell (L02) for OPMS modified NLC, and the highest uptake was observed for 5×10^{-3} mmol of OPMS modified one. No obvious difference was found among the L02 uptake of OPMS modified NLCs and NLC, but their uptake was higher than that of PGMS modified NLCs. All the results indicated that the OPMS highly modified NLCs would improve the effect of antitumor therapy by inhibiting the degradation, evading RES and enhancing the drug uptake of tumor cells.

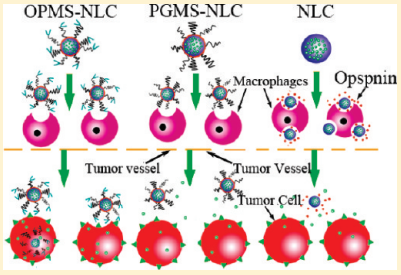

KEYWORDS: polyethylene glycol(100) monostearate, octreotide, somatostatin receptor, nanostructured lipid carrier

INTRODUCTION

The objective of cancer chemotherapy was to achieve site-specific drug delivery as well as minimize systemic side effects. Ligand−PEG-lipid conjugate was widely used as targeting molecule in drug delivery systems (DDS).[1] Each part of the conjugate played a different role. As an active targeting molecule, the ligand increased the affinity of DDS for the target site. The hydrophilic PEG segment might prolong the systemic circulation time and minimize the nonspecific interaction with nontarget sites such as the reticuloendothelial system (RES). The hydrophobic lipid was generally utilized as an anchor molecule connecting the conjugate with DDS. Lots of examples were found in ligand−PEG-lipid based targeted liposomes for cancer drug delivery and achieved tumor targeting both in vitro and in vivo.[2,3]

It was reported that somatostatin receptors (SSTRSs) had been investigated as potential targets because they were over-expressed in some tumors.[4] Somatostatin analogues including octreotide, lanreotide, vapreotide etc. conjugated to radioactive isotopes or cytotoxic drugs had been used for tumor diagnosis and therapy.[5,6] For example, [^{125}I][Tyr^3]octreotide,[7] indium-111 DTPA octreotide (OctreoScan),[8] 90Y−DOTATOC (beta-emitter yttrium-90 conjugated via DOTA to Tyr3-octreotide (DOTATOC)),[9] octreotide conjugated paclitaxel,[10,11] somatostatin AN-238 consisting of 2-pyrrolinodoxorubicin (AN-201) linked to a somatostatin analogue RC-121[11] and camptothecin-somatostatin (CPT−SS) conjugates[12] had all been proved usefully to explore the efficacy of receptor-mediated cytotoxicity and selectively destroy cancer cells while sparing normal tissues. In consideration of the pharmaceutical setting, octreotide as the tumor targeting ligand possessed specific affinity for SSTR-2 and SSTR-5[13] and high stability in physiological conditions. Sun et al.[14] and Zhang et al.[15] had successfully conjugated octreotide to the PEG end of PEG-PE or PEG-DSPE; however the final products were often a mixture, containing several non-site-specific conjugates of the peptide−PEG-lipid and nonreacted PEG-lipid, and the yield was somewhat low. These gave birth to an idea of using octreotide as the targeting moiety to develop a novel, simplified octreotide−PEG-lipid conjugate, which would be of

Received: December 30, 2010
Accepted: July 19, 2011
Revised: July 12, 2011
Published: July 19, 2011

benefit to improve the site-specification, purification and yield as well as protect the functional groups.

Nanostructured lipid carrier (NLC) consisting of solid lipid and liquid lipid was a new type of colloidal drug delivery system, which offered advantages of improving drug loading capacity, controlling release properties and drug targeting.[16−19] Taking the physiological and/or biodegradable lipids into consideration, NLC also revealed an excellent tolerability compared with polymeric nanoparticles; furthermore, NLC was easier to scale up, more stable for storage and less costly than liposomes. By now NLC was mainly investigated for dermal application with few investigations focusing on the parenteral route.[20] In this paper, efforts were focused on improving the drug targeting efficiency of NLCs, especially aiming to enhance the stability, prolong the retention of drug in vivo and enhance the drug uptake of tumor cells.

Polyethylene glycol(100) monostearate (PGMS) with polyethylene glycol (PEG) molecular weight 4000 g/mol was an amphiphilic polymeric derivative of hydrophilic PEG modified by attaching a hydrophobic moiety, which could be easily incorporated into the lipid core of NLC with the hydrophilic PEG chains on their surface.[21,22] In current studies, octreotide was conjugated with PGMS to obtain octreotide−PEG-monostearate conjugate (OPMS) using a two-step method which was site-specific and high yield and did not interfere with biological activities of octreotide. Then 10-hydroxycamptothecin (HCPT), a derivative of natural camptothecin (CPT) which had been shown to be more active and less toxic against gastric carcinoma, hepatoma, leukemia and tumor of head and neck as compared with CPT,[23] was chosen as the model drug to construct HCPT-loaded NLC. In addition, current research suggested the thermodynamic stability, prolongation of the circulation half-life and cellular uptake of colloidal drug delivery systems were influenced by the amounts of PEG modification.[22,24,25] Therefore, the effects on different amounts of PGMS and OPMS used to modify NLCs were investigated in order to evaluate physicochemical properties, plasma stability, pharmacokinetics and cellular uptake.

MATERIALS AND METHODS

Materials. 4-Nitrophenyl chloroformate was obtained from Suzhou Time-Chem Technologies Co. Ltd. (China). Octreotide was purchased from Shanghai C-Strong (China). Polyethylene glycol(100) monostearate (PGMS) with PEG molecular weight 4000 g/mol was purchased from Sigma (Milwaukee, WI, USA). HCPT (purity 99.0%) was provided by Knowshine (Shanghai) Pharmachemicals Inc. (China). Soybean phospholipids (PC, purity 90%) were a kind gift from Evonik Degussa China Co., Ltd. (Shanghai, China). Labrafac CC was kindly gifted from Gattefosse. Trilaurin and coumarin-6 were purchased from Tokyo Chemical Industry (TCI, Japan). RPMI-1640 cell culture medium was from Gibco (Life Technologies, Switzerland). 3-(4,5-Methylthiazol-2-yl)-2,5-diphenyltetrazolium bromide (MTT) was obtained from Amresco (Solon, Ohio, USA). BCA Protein Assay Kit was from Thermo Scientific Pierce (Rockford, USA). The other reagents were analytical grade and used without further purification. Double distilled water was used in this study.

Animals. Sprague−Dawley (SD) rats were obtained from the Shanghai Silaike Laboratory Animal Ltd., were housed on standard laboratory diet at an ambient temperature and humidity in air-conditioned chambers and were used for the present studies. All the animals were pathogen free and allowed to access food and water freely. All animal experiments were conducted in full compliance with local, national, ethical and regulatory principles with the approval of the Institutional Animal Care and Use Committee at China Pharmaceutical University.

Cell Cultures. The following cell lines were used: L02 (human-derived liver cell), SMMC-7721 (human hepatocellular carcinoma cell line). Both of them were grown in RPMI1640 supplemented with 10% (v/v) fetal bovine serum. Cells were incubated in a humidified atmosphere at 37 °C, gassed with 5% CO_2 in air, and subcultured every 2 days with 0.25% trypsin.

Synthesis of Octreotide−Polyethylene Glycol-Monostearate Conjugates (OPMS). OPMS was synthesized with a two-step procedure. The first step was according to previous research with a little modification[26] and formed a new amphiphilic intermediate, *p*-nitrophenylcarbonyl-Polyethylene glycol(100) monostearate (pNP-PGMS).

Second, 50 mg of pNP-PGMS was dissolved in 5 mL of dichloromethane; then the organic solvent was evaporated until complete dryness under vacuum and formation of a dried film. 11 mg of octreotide dissolved in 4 mL of 0.01 mol/L HCl was added to the dried film, homogenized by sonication to obtain suspension and then mixed with 20 mL of 0.2 mol/L $NaCO_3$−$NaHCO_3$ buffer (pH 9.0). The mixture was incubated for about 12 h at 4 °C and dialyzed with a Spectrum dialysis bag (MWCO of 5 kDa, BBI, Canada) at 4 °C for 48 h to remove free octreotide. Finally, OPMS solution was lyophilized and stored at 4 °C until further use. The structure of the conjugate was characterized by ^{1}H NMR spectrum, surface tension measurement and synchronous fluorescence spectra (SFS).[27]

Determination of Coupling Ratio of Octreotide on PGMS. The amount of octreotide on the OPMS was determined via BCA Protein Assay Kit. In brief, the amount of octreotide was calculated from a standard curve obtained from the octreotide solutions mixed with PGMS as standard solution in a series of concentrations (25−500 μg/mL). 20 μL of OPMS solution after dialyzing or above standard solution and 200 μL of BCA WR were added into a 96-well plate and mixed completely. After incubation for 30 min at 37 °C in the dark, the absorbance was measured at 570 nm on a Microplate Reader (Thermo Electron Co.). The above procedure was performed in triplicate. The coupling ratio (CR) of reaction was calculated with the following formula:

$$CR(\%) = CV/Q \times 100\%$$

where CR is coupling ratio of reaction, C is the concentration of coupled octreotide in OPMS solution after dialyzing, V is the volume of OPMS solution after dialyzing and Q is the amounts of octreotide added into the reaction.

Preparation of HCPT-Loaded NLCs. The solvent evaporation method as described by Lu et al. and Nikanjam et al.[28,29] was utilized to prepare NLC with some modifications. In a 0.5 L round-bottomed flask, lipid matrix materials and HCPT were dissolved in 20 mL of ethanol−methylene dichloride solvent mixture (8:2, v/v). Lipid matrix containing PC, Trilaurin, Labrafac CC and vitamin E were fixed at an optimized mass ratio of 66.3:24.1:4.8:4.8 (w/w). Meanwhile, HCPT was 2.5 wt % of lipid matrix. The organic solvent was evaporated under vacuum at 40 °C for 4 h, and then the flask was placed in desiccators under vacuum overnight. The dried lipid film was hydrated with 2.6% (v/v) glycerol solution at 37 °C for 30 min and ultrasonicated at

Scheme 1. Schematic Representation of the Unmodified and Modified NLCs

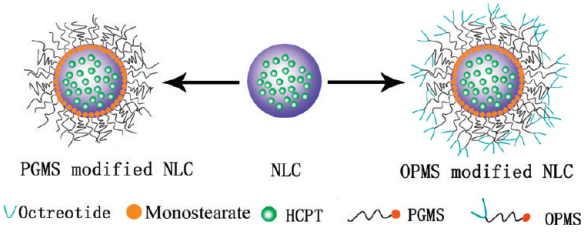

400 W for 15 min. The unentrapped drug was removed using a 0.22 μm cellulose nitrate membrane.

For the preparation of modified NLCs, PGMS or OPMS was added into the lipid matrix and then the procedures were the same as those described above. Two different amounts of PGMS or OPMS, 2×10^{-3} mmol and 5×10^{-3} mmol of each, were added into the matrix to evaluate the effect of modification amounts on characterization, drug release and other properties of NLCs. Correspondingly, based on the modification of agents and their amounts, the modified NLCs were named in order as P_L-NLC, P_H-NLC, O_L-NLC and O_H-NLC, respectively (Scheme 1).

Particle Size, Zeta Potential and Morphology. Particle size, its distribution indicated by polydispersity index (PI) and zeta potential of HCPT-loaded NLC were determined by Zetasizer 3000HS (Malvern, U.K.). The morphological observation was performed under transmission electron microscopy (TEM, H-600, Hitachi, Japan) following negative staining with 0.1 wt % sodium phosphotungstate solution. Additionally, atomic force microscopy (AFM) (Veeco diNanoScope V, USA) was also used to characterize the morphology. The samples of AFM were made according to the following description: one drop of properly diluted nanoparticle suspension was placed on the surface of a clean silicon wafer and air-dried at room temperature. Then the sample was observed by AFM with a 5 μm scanner in contact mode.

Determination of Encapsulation Efficiency (EE) and Drug-Loading Coefficient (DL). The concentration of HCPT in unmodified NLC and modified NLCs was determined by Shimadzu 10-A vp HPLC system (Kyoto, Japan). The stationary phase, Diamonsil C_{18} column (150 mm ×4.6 mm, 5 μm), was kept at 40 °C. The mobile phase was a mixture of 55:45 methanol:0.075 mol/L ammonium acetate buffer (v/v, pH 6.5) adjusted with acetic acid. The flow rate was 1.0 mL/min. The injection volumn was 20 μL, and effluent was monitored at 383 nm. HPCT-loaded NLCs were filtrated through the 0.22 μm cellulose nitrate membrane. The 50 μL filtration was dissolved in 450 μL methanol and vortexed for 30 s, and then centrifuged at 12,000 rpm for 10 min. The drug concentrations before and after filtration were determined. EE in the NLCs was calculated as follows:

$$EE(\%) = (C_a/C_b) \times 100\%$$

where C_a is the concentration of the drug after filtration and C_b is the concentration of the drug before filtration.

DL in the NLCs was calculated as follows:

$$DL(\%) = Q_d/(Q_d + Q_m) \times 100\%$$

where Q_d is the amounts of the drug in NLCs and Q_m is the amount of the feeding materials.

Calculation of Fixed Aqueous Layer Thickness (FALT) of NLCs. The FALT was calculated via Gouy−Chapmann theory.[30] According to this theory, zeta potential $\psi(L)$ as the electrostatic potentials at the position of the slipping plane L was expressed as

$$\ln \psi(L) = \ln A - kL$$

where A is a constant and k is the Debye−Huckel parameter, equal to $\sqrt{(C)}/0.3$ (C is the molality of electrolytes). If zeta potentials were measured from the changing concentrations of NaCl (0, 0.01, 0.05, 0.1 M, respectively) and plotted against k, the slope L gave the position of the slipping plane or thickness of the fixed aqueous layer in nm units.

Determination of Incorporated Ratio (IR) of PGMS and OPMS, Average Surface Density of PEG (SD_{PEG}) and Distance (D) between Two Neighboring PEG Grafting Sites of Modified NLCs. The amounts of nonadhered PGMS or OPMS, defined as W_1, were obtained by ultrafiltration with molecular weight cutoff 100 kDa and determined by colorimetric method as described by Peracchia et al.[31] with a slight modification. PEG content was calculated by a standard curve in a range from 1 to 15 μg PEG/mL. The amounts of total PEG in modified NLCs (including the nonadhered and adhered PEG on the surface of NLC), defined as W_2, were directly measured without ultrafiltration. Thus, the amounts of PEG attached on the surface of NLC were equal to $(W_2 - W_1)$ and the incorporation ratio (IR) of PGMS and OPMS was calculated by

$$IR(\%) = (W_2 - W_1)/W_2 \times 100\%$$

The surface density of PEG chains (SD_{PEG}) could be defined by the ratio between the total number of PEG chains (N_{PEG}) and the nanoparticle surface area (S_{np}):[31]

$$SD_{PEG} = N_{PEG}/S_{np}$$

Resolving, $N_{PEG} = (W_{PEG}/MW_{PEG})A_n$, where W_{PEG} is equal to $(W_2 - W_1)$, MW_{PEG} is the molecular weight of PEG and A_n is Avogadro's number. $S_{np} = 4\pi r^2 N_{NLCs}$, N_{NLCs} is the total number of nanoparticles and r is approximate to the whole particle radius, neglecting the PEG layer thickness (error < 10%). From these data of SD_{PEG}, the D was calculated by

$$D = \sqrt{1/SD_{PEG}}$$

In Vitro Drug Release of NLCs. In vitro drug release of NLCs with plasma or without plasma was analyzed by a membrane dialysis technique. In order to investigate stability of NLCs in the acidic microenvironment of the tumor, the study of drug release in vitro was done in phosphate buffer with pH 7.4, pH 6.5 and pH 5.4. 1 mL of NLCs (containing 500 μg of HCPT) was placed into a preswelled dialysis bag (3.5 kDa MW cutoff, Sigma, USA). Meanwhile, HCPT solution was prepared as control. To simulate the in vivo environment, 1 mL of fresh rat plasma was placed into the dialysis bag. The bag was tightened and soaked in 150 mL of phosphate buffer. The HCPT concentration was kept at a level lower than the solubility of HCPT in phosphate buffer (about 9 μg/mL) through all the experiment. The experiments were carried out at 37 °C for 48 h in 3 replicates. At predetermined intervals, 5 mL of the dissolution medium was withdrawn and replaced with the same amount of prewarmed fresh medium.

The samples of the replicates were acidified with glacial acetic acid before analysis by HPLC.

Influence of Rat Plasma on Particle Size, PI and Drug Release of NLCs. In this part of the study, 3 mL of each NLC suspension was mixed with 3 mL of fresh rat plasma at 37 °C with soft stirring. After the specified incubation time, 100 μL of mixture was withdrawn and determined by Zetasizer 3000HS. Meanwhile, another 200 μL of mixture was applied on the top of a 1 cm × 40 cm column, filled with 10 mL of Sephadex G50. Then the column was eluted at a flow rate of 1 mL/min with phosphate buffer pH 5.6. Sample fractions from 7 to12 mL were collected, demulsified by methanol (1:9, v/v) and acidified with glacial acetic acid before analysis by HPLC. The change of particle size was calculated as follows:

$$change\ of\ particle\ size\ (\%) = [size(0) - size(t)]/size(0) \times 100\%$$

where size(0) is the value of size before incubation and size(t) is the value of size after t min incubation time.

The change of size distribution was calculated as follows:

$$change\ of\ PI\ (\%) = [PI(t)/PI(0) - 1] \times 100\%$$

where PI(0) is the value of PI before incubation and PI(t) is the value of PI at t min.

The ratio of drug release from NLCs was calculated as follows:

$$drug\ release\ (\%) = [EE(0) - EE(t)]/EE(0) \times 100\%$$

where EE(0) is the value of EE before incubation and EE(t) is the value of EE at t min.

Pharmacokinetics Studies in Rats. The in vivo concentration of HCPT in plasma was determined as describe in Determination of Encapsulation Efficiency (EE) and Drug-Loading Coefficient (DL) except that HCPT was monitored by a fluorescence detector (Shimadzu, Japan) with excitation wavelength of 382 nm and emission wavelength of 528 nm. Once drawn, the sample was centrifuged at 4000 rpm for 10 min at 4 °C. The plasma was frozen at −20 °C until assay. 10 μL of glacial acetic acid and 200 μL of ethyl acetate:methanol (1:1, v/v) were added into 100 μL of plasma and vortexed for 2 min. The mixture was centrifuged at 12000 rpm for 10 min, and 20 μL of supernatant was injected into the HPLC system. The HCPT-loaded NLCs were used in this experiment, and HCPT injection acted as reference. All the preparations were administered intravenously into the tail vein of male SD rats at a dose of 2.5 mg of HCPT/kg (n = 6), and blood samples were taken with a heparinized syringe at 5, 15, 30, 60, 120, 240, 480, 720, and 1440 min. The plasma concentrations versus time data were analyzed by Kinetica 4.4 (Thermo Electron Corporation, Waltham, MA, USA). Parameters including $t_{1/2}$, MRT and AUC were determined.

Cellular Uptake Study by Fluorescent Microscopy. In this study the NLC loading coumarin-6 was prepared by the method as described in Preparation of HCPT-Loaded NLCs, but HCPT was replaced with coumarin-6. L02 and SMMC-7721 were seeded at a density of 10^5 cells/well on a pretreated coverslip. After 24 h, cells were incubated with HBSS for 20 min. Next, the medium was replaced with NLC samples in which the concentration of coumarin-6 was 500 ng/mL and incubated for 2 h. After removing the supernatant and washing the well three times with PBS7.4, cells were fixed by 4% paraformaldehyde for 20 min. Then, they were rinsed three times with PBS7.4 and observed under fluorescent microscope (Olympus X 51, Japan).

Statistical Data Analysis. Statistical data analysis was performed using the Student t test with $p < 0.05$ as the minimal level of significance.

RESULTS AND DISCUSSION

Synthesis and Characterization of Octreotide−Polyethylene Glycol(100) Monostearate (OPMS). The OPMS was synthesized and confirmed by ^{1}H NMR spectrum. The surface tension and SFS identification revealed that the hydrophilicity of PEG and the local microenvironment of Trp of octeotide were not changed after the coupling reaction. The coupling ratio of octreotide on the PGMS of three batches of products determined by BCA Protein Assay Kit was 89.17 ± 2.79% (n = 3). Numerous coupling strategies had been developed to achieve site-directed ligand−PEG-lipid conjugates.[1,14,15,32] There were two amino groups in the structure of octreotide, α-amino group and ε-amino group, and the latter was the active site of octreotide. In order to conjugate with α-amino group selectively, the pH of the reaction had to be carefully maintained below 10 as described by Sun et al.[14]

Preparation and Characterization of NLCs. The particle size, PI and zeta potential are listed in Table 1. The modification of PGMS or OPMS resulted in decreasing of the particle size as compared with NLC, which might be due to the increase of surface-active effect with mixing surfactant.[33] In addition, the PEG chain of these systems could act as a tighter net on the outside of vesicles, thus limiting the increase of vesicle size.[34] According to the previous report, it was possible for nanoparticles with size around 100−200 nm to exhibit long blood circulation effect due to avoidance of the recognition of RES and accumulate in tumors via "leaky" vasculature through the enhanced permeability and retention (EPR) effect.[35,36]

From Table 1 it was observed that the value of zeta potential of NLCs was increased by modifying different amounts of PGMS and OPMG because the presence of PEG on the surface of nanoparticles partially masked the negative charge.[19,37] The higher the amounts of PGMS and OPMG were, the less the negative value of zeta potential was. After a complete screening of the surface by PEG attachment, the zeta potential would be practically zero, which was considered sufficient to avoid RES recognition.[36] Moreover, a zeta potential range of −20 to −11 mV corresponds to the threshold of agglomeration in dispersion.[33] Thus the range of zeta potential obtained in this study was not high enough for a sufficient electrostatic stabilization. However, PGMS and OPMS, containing PEG chains, could provide additional steric stabilization for modified NLCs.

Figure 1 shows the TEM of unmodified and modified NLCs. It could be observed that unmodified NLC appeared as spherical shapes (Figure 1A) and modified NLCs exhibited quasi-spherical shapes (Figure 1B). The border of unmodified NLC might be surrounded by single or more phospholipid layers, while modified NLCs showed a core/shell structure with PEG chains dangling outside of NLCs and providing steric stabilization to the vesicle. The particle size measured by TEM was smaller than that measured by Zetasizer 3000HS. This could be attributed to the fact that Zetasizer 3000HS measured the hydrodynamic diameter of vesicles, for which the PEG chain had significant effect on vesicle size; while TEM measured the vesicles adsorbed on a copper screen under vacuum condition.

Figure 2 shows the AFM of unmodified and modified NLCs. Both of them appear as quasi-spherical shapes. As shown by curves A and B, the particle size measured by AFM was larger

Table 1. Physicochemical Properties of NLCs[a]

preparations	PGMS (mmol)	OPMS (mmol)	size (nm)	PI	zeta potential (mV)	EE (%)	DL (%)
NLC			121.4 ± 2.5	0.26 ± 0.03	−15.04 ± 1.03	94.4 ± 3.7	2.2 ± 0.13
P_L-NLC	2×10^{-3}		119.6 ± 1.8	0.23 ± 0.08	−6.54 ± 0.98	95.2 ± 4.4	2.2 ± 0.15
P_H-NLC	5×10^{-3}		103.6 ± 3.3	0.31 ± 0.04	−5.76 ± 2.01	90.7 ± 3.8	1.9 ± 0.12
O_L-NLC		2×10^{-3}	120.5 ± 1.7	0.25 ± 0.06	−3.77 ± 1.17	93.6 ± 5.5	2.2 ± 0.18
O_H-NLC		5×10^{-3}	113.7 ± 2.4	0.30 ± 0.07	−3.74 ± 1.25	91.4 ± 4.8	1.9 ± 0.15

[a] Data are represented as mean ± SD (n = 3).

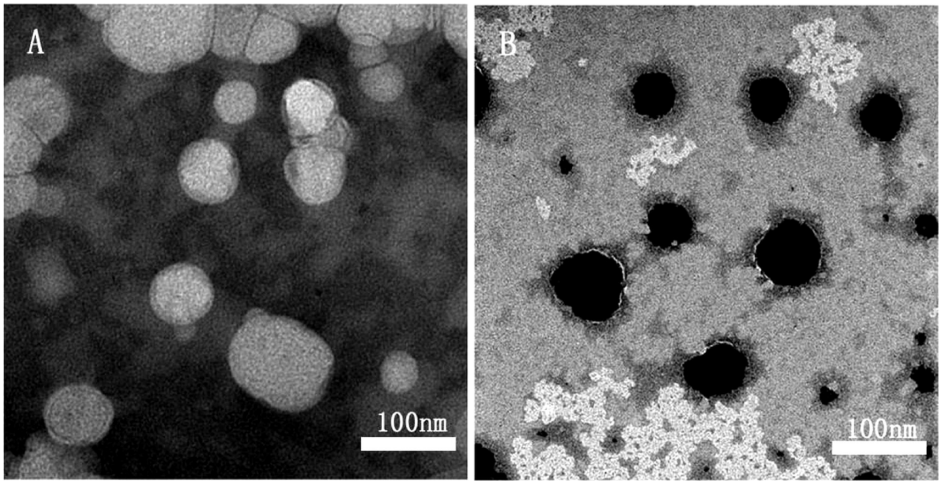

Figure 1. The TEM of unmodified NLC (A) and modified NLC (B).

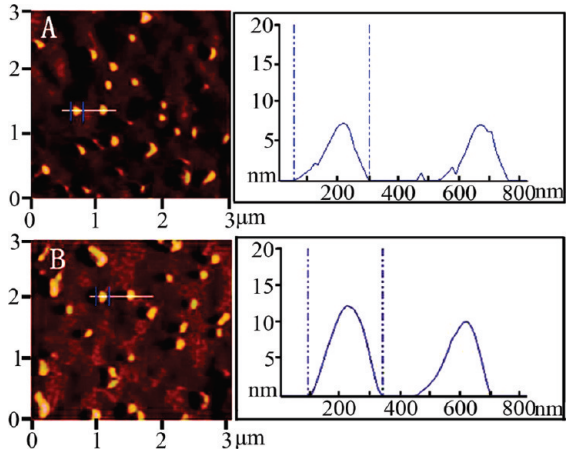

Figure 2. AFM images of unmodified NLC (A) and modified NLC (B). The profiles were obtained from the height images.

than that measured by Zetasizer 3000HS and the geometric diameter of unmodified and modified NLCs was almost 2 times larger than that of Zetasizer 3000HS. It might be responsible for lipid spreading or flattening of NLCs onto the mica surface and fusion process during sample preparation.[38−40] The height of modified NLC measured from AFM images was higher than that of unmodified, 12 nm vs 7 nm, and the X/Z curve of modified NLCs appeared smooth, but the X/Z curve of unmodified NLC was crude, which could further confirm the fact that the PEG chains served as a rough shell or "coating" outside NLCs.[34]

Table 2. FALT, IR, SD_{PEG} and D for NLCs[a]

preparations	FALT (nm)	IR (%)	SD_{PEG}	D (nm)
NLC	0.80 ± 0.31			
P_L-NLC	1.74 ± 0.57#	85.69 ± 0.77	0.187 ± 0.024	2.45 ± 0.04
P_H-NLC	2.38 ± 1.02#	78.50 ± 1.82*	0.492 ± 0.019*	1.42 ± 0.03*
O_L-NLC	2.19 ± 0.87#	84.06 ± 1.15	0.220 ± 0.015	2.17 ± 0.02
O_H-NLC	3.72 ± 0.45#*	74.71 ± 0.79*	0.592 ± 0.021**	1.30 ± 0.03*

[a] Data are represented as mean ± SD (n = 3). #$P < 0.05$, versus NLC; *$P < 0.05$, versus P_L-NLC and O_L-NLC; **$P < 0.05$, versus P_L-NLC, O_L-NLC and P_H-NLC.

Fixed Aqueous Layer Thickness (FALT). As shown in Table 2, with increasing the amounts of PGMS and OPMS from 2×10^{-3} to 5×10^{-3} mmol, the FALT increased. The results were in good agreement with the reports. Shimada et al.,[41] Sadzuka et al.[42] and Shi et al.,[43] who found that FALT was a function of PEG molecular weight and the amounts of PEG used. The FALT suggested that the PEG chains of PGMS and OPMS constructed more complete "mushroom" structures than "brush" structures according to the modeling of PEG-lipid by Needham et al.[44] On the one hand, in the "brush" model, the FALT was more than 10 nm.[30]On the other hand, the transition of conformation from mushroom to brush was predicted to occur at less than 2 mol % for PEG5K-Lipid, while at least 60 mol % of PEG5K-Lipid in the brush conformation was needed to fully cover the surface.[45−47] In present studies, the grafting density of PGMS in P_L-NLC and P_H-NLC was 1.2 mol % and 2.8 mol %, and the grafting density of OPMS in O_L-NLC and O_H-NLC was 1.2 mol % and 2.7 mol %, respectively. Therefore, the conformation of PEG chains in the

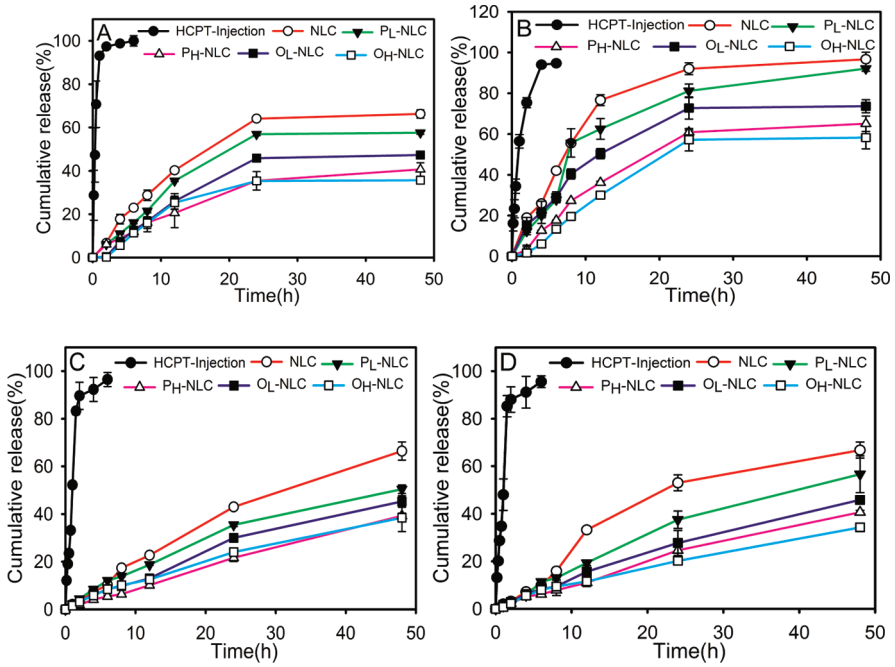

Figure 3. In vitro release curve of HCPT from HCPT injection and HCPT-loaded NLCs: (A) pH 7.4 without plasma, (B) pH 7.4 with plasma, (C) pH 6.5, (D) pH 5.4 (n = 3).

surface of modified NLCs was located somewhere between the "mushroom" and "brush". This meant that most of the PEG chains constricted slightly and possessed enough density to ensure that no gaps or spaces on the particle surface were left uncovered.[48]

Surface Properties of Modified NLCs: IR, SD_{PEG} and *D*. As has been shown in Table 2, OPMS modified NLCs showed lower IR but higher SD_{PEG} compared with PGMS modified NLCs at the same amounts of modified materials. When modified with 2×10^{-3} mmol of PGMS or OPMS, the IR was higher than that modified with 5×10^{-3} mmol ($P < 0.05$), but the SD_{PEG} was lower than that modified with 5×10^{-3} mmol ($P < 0.05$). PGMS and OPMS both had the same hydrophobic "anchor", stearin, but with different molecular weight of hydrophilic chains. As the length and flexibility of hydrophilic chains increased, the hydrophilic interaction between hydrophilic chain and aqueous medium was stronger than that of hydrophobic interaction between the hydrophobic "anchor" and the core.[49,50] In addition, further increasing the amounts of PGMS and OPMS led to the reduction of IR, which should be attributed to a sterical hindrance of the reactivity by hydrophilic chains. Thus the conclusions could be drawn that the incorporation of OPMS was more difficult than that of PGMS and had lower incorporated ratio.

Moreover, previous research proved that SD_{PEG} depended on not only the IR but also the molecular weight of hydrophilic chains and particle size.[51,52] In order to reach the same SD_{PEG}, the higher the molecular weight of the hydrophilic chains was, the less amount of PEG-lipid was needed; besides SD_{PEG} decreased with the descent of particle size due to the larger specific surface area of nanoparticles for partition of PEG chains. So in this study the SD_{PEG} might be influenced by all of the above factors.

In this study the *D* of P_L-NLC and O_L-NLC was 1.72-fold and 1.67-fold wider than that of P_H-NLC and O_H-NLC. With increasing the modified material from 2×10^{-3} and 5×10^{-3} mmol, the *D* decreased, which meant that the PEG on the surface of NLCs got thicker and narrowed the distance between two neighboring PEG grafting sites of modified NLCs. As reported by Gref, the radius of most of the plasma proteins was between 2 and 5 nm.[53] So when modified with 2×10^{-3} mmol of PGMS and OPMS it was not enough to prevent the adsorption of proteins, but the capacity of decreasing protein adsorption strengthened when the amounts of PGMS and OPMS reached 5×10^{-3} mmol.

In Vitro Release of HCPT-Loaded NLCs. In vitro release study was shown in Figure 3. Except for HCPT-injection, all preparations did not exhibit a fast release of HCPT at the initial stage, which could be attributed to the encapsulation of HCPT into NLCs and the depot effect of NLCs. Comparing Figure 3 panels A and B, it was observed that the release rate increased in the present of plasma. The faster release might be due to the increase of solubility of HCPT in plasma and accelerated passive diffusion of HCPT from the lipid core of NLCs; besides the faster release might be also due to the degradation of NLC lipid matrix by all kinds of lipase in plasma[54−56] and increase the speed of the hydration of the drug molecules in the inner core with release medium. The sustained release effect of modified NLCs is better than that of NLC, and the higher amounts of modified materials were applied, the better sustained release effect was obtained. With the same amounts of modified materials OPMS modified NLCs showed a slower release rate than that of PGMS modified NLCs. It was likely that the sterical hindering effect of PGMS and OPMS abated the adsorption of lipase on the surface of modified NLCs and slowed down the degradation. Comparing Figure 3 panels A, C and D, the release behavior of HCPT-loaded NLCs in pH 6.5 and 5.4 was similar to that in pH 7.4. Therefore, NLCs could maintain significantly sustained release behavior under the microenvironment of tumor.

In order to speculate the release mechanism of HCPT-loaded NLCs, several popular kinetic models were used to simulate all the release profiles, including the zero-, first-, Higuchi release models, Hixson−Crowell cube root model (H−C), Weibull

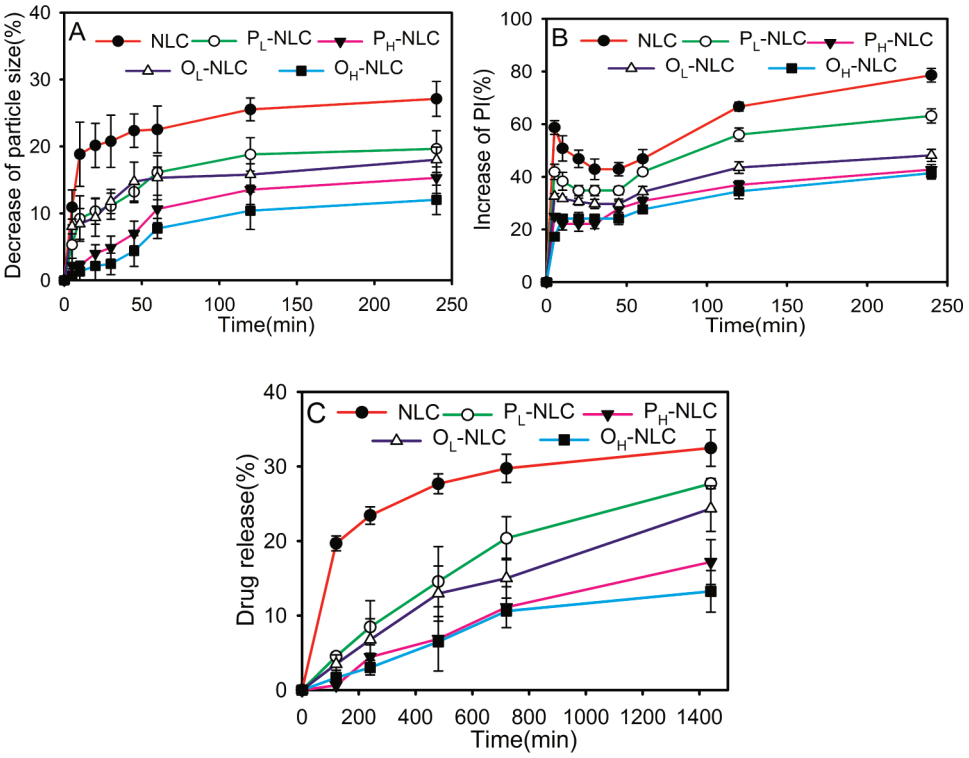

Figure 4. Influence of plasma on particle size, PI and drug release of NLCs: (A) the particle size change curve of NLCs; (B) the PI change curve of NLCs; (C) the drug release of NLCs (n = 3).

model, and the novel reciprocal powered time model (RPT).[57−59] Akaike's approach and AIC (Akaike discriminatory criterion) values were applied to determine the suitability of these models.[60] According to the minimum values principle of AIC, the Weibull and RPT models were found to be much better for the simulation of all release profiles than other models, although the H−C model also gave smaller AIC values, especially while the plasma was in pH 7.4 PBS. The H−C model mainly implied an erosion process;[57,58] obviously, the presence of various enzymes in plasma could accelerated the particle erosion. However, Barzegar−Jallali et al.[59] had reported that both the Weibull and RPT models could be applicable for any release mechanisms of drug-loaded nanoparticles, such as dissolution, diffusion, mixed dissolution−diffusion and erosion. Therefore, our results suggested that several mechanisms may be involved in the HCPT release from NLCs other than a single erosion process. The penetration of liquid media into the system, hydration and passive diffusion might also play a role. The AIC values of the three model simulations for in vitro release profiles of HCPT-loaded NLCs in different PBS media and in pH 7.4 PBS with plasma are summarized in Tables SI1−SI4 in the Supporting Information.

Influence of Plasma on Particle Size, PI and Drug Relaese of NLCs. Goppert and Muller[61] demonstrated that in the first 5 min after iv administration up to 90% of the injected dose was recognized by the MPS and taken up by the liver macrophages; if particles "survive" this first 5 min, prolonged blood circulation was found. Figure 4A illustrates the particle size change curve of NLCs. During the first 5 min the particle size of NLC, P_L-NLC and O_L-NLC decreased 10.92%, 5.30% and 8.02% respectively. However, plasma had less effect on P_H-NLC and O_H-NLC: only 2.22% and 0.71% of decrease were observed. The change of particle size might be responsible for two aspects: the surface degradation of NLCs leading to a decrease in particle size and the plasma protein adsorption resulting in an increase in particle size. Obviously, the effect of surface degradation on the particle size played a greater part than plasma protein adsorption.

Figure 4B reveals that the PI rose sharply after 5 min incubation time except for O_H-NLC, and then slowed down with increasing incubation time. Subsequently, no obvious increase of PI was observed after 60 min incubation time except for NLC. This phenomenon could be explained by the adsorption of plasma protein on the surface of NLCs. According to the "Vroman effect" the plasma protein adsorption was time-dependent.[62] At the first 5 min plasma proteins with high concentrations but lower affinity in plasma would initially occupy the surface of the nanoparticle to cause a rapid change of particle size.[63] As shown in Figure 4A, with incubation time prolonging the decrease of particle size allow the surface areas of nanoparticles to shrink much more slowly than their volumes, causing nanoparticles to have far greater surface-to-volume ratios and to be able to bind more plasma protein than before. So the effect of plasma protein adsorption on particle size became slight.

Figure 4C shows that the drug release from NLCs rose gradually as incubation time expanded. After 24 h incubation, the percentage of drug release from NLC reached 32.48%, which was 1.17-, 1.89-, 1.33-, and 2.45-fold of that of P_L-NLC, P_H-NLC, O_L-NLC and O_H-NLC respectively. Apart from the degradation of plasma, the increase in solubility of HCPT in plasma also accelerated the drug release from NLCs. The protection of modified materials was amount-dependent. As shown above, the more the modified materials were used, the higher SD_{PEG} and the narrower D were acquired. All above would lead to strengthen the effect of protection and

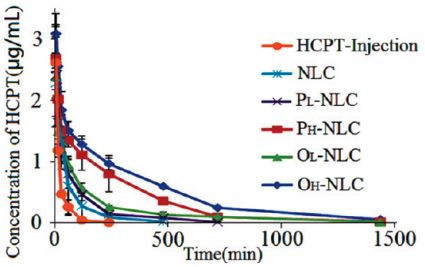

Figure 5. Concentration−time curve of HCPT in rat plasma after iv administration of HCPT injection, NLC, P_L-NLC, P_H-NLC, O_L-NLC and O_H-NLC (n = 6).

Table 3. Pharmacokinetics Parameters of HCPT Injection, NLC, P_L-NLC, P_H-NLC, O_L-NLC and O_H-NLC after Iv Administration[a]

preparations	$t_{1/2}$ (min)	MRT (min)	AUC (μg min/mL)
HCPT injection	34.37 ± 4.01	39.03 ± 4.02	57.84 ± 7.81
NLC	104.9 ± 15.41$^{\#}$	101.58 ± 13.62$^{\#}$	134.95 ± 32.93$^{\#}$
P_L-NLC	123.35 ± 29.19$^{\#}$	153.17 ± 21.27$^{\#*}$	185.59 ± 18.69$^{\#}$
P_H-NLC	240.88 ± 22.23$^{\#**}$	298.97 ± 13.47$^{\#**}$	510.12 ± 27.49$^{\#**}$
O_L-NLC	146.94 ± 12.37$^{\#*}$	176.50 ± 16.50$^{\#*}$	252.92 ± 14.32$^{\#*}$
O_H-NLC	313.26 ± 8.91$^{\#***}$	395.92 ± 10.40$^{\#***}$	731.44 ± 36.45$^{\#***}$

[a] Data are represented as mean ± SD (n = 6). $^{\#}P < 0.05$, versus HCPT injection; $^{*}P < 0.05$, versus NLC; $^{**}P < 0.05$, versus NLC, P_L-NLC and O_L-NLC; $^{***}P < 0.05$, versus NLC, P_L-NLC, O_L-NLC and P_H-NLC.

NLC modified by OPMS also revealed the better effect of protection.

Pharmacokinetic Studies in Rats. Figure 5 depicts the plasma concentration−time profiles after intravenous injection in rats. Encapsulation of HCPT into NLCs dramatically increased the mean residence time (MRT) and the area under the curve (AUC) compared with HCPT injection ($P < 0.05$). In fact, after 4 h the concentrations of HCPT in NLC, P_L-NLC, P_H-NLC, O_L-NLC and O_H-NLC in blood were about 4.10, 10.92, 58.64, 20.01 and 67.19 times that of free HCPT. Then the free HCPT was quickly removed from the circulating system and could not be detected. On the contrary, P_H-NLC and O_H-NLC exhibited a remarkable retention with the drug levels of 15.8 and 58.5 ng/mL at 24 h.

Comparing the pharmacokinetic parameters of NLC and modified NLCs, an even higher MRT and AUC were observed for the latter, confirming the protective effects of PGMS and OPMS (Table 3). Meanwhile, the long circulative effect of modified NLCs was depended on the amounts of PGMS or OPMS used. All above were in agreement with the results of surface properties, in vitro release and plasma stability studies, which meant the dominant mechanism of prolonged retention of modified NLC was to inhibit the degradation and evade RES uptake after entering the systemic circulation.

In this study, OPMS modified NLCs seemed to have superior stealth effects compared with PGMS modified NLCs at the same amounts of modified materials used. There were several reasons for this result: For the long-circulating effect it was necessary to have a less negative or even neutral zeta potential.[53] As shown in Table 1, OPMS modified NLCs possessed less negative zeta potential in contrast to PGMS modified NLCs ($p < 0.05$). Second, FALT was an important factor for improving stability, preventing opsonization and macrophage uptake. Our above study proved that the FALT of OPMS modified NLCs was thicker than that of PGMS modified NLCs at the same amounts of modified materials. Third, the optimal SD_{PEG} close to 0.5−0.67 PEG/nm^2 for one PEG is suggested for avoiding complement consumption, and the D should be around 1−1.5 nm to avoid the adsorption of proteins.[36,64] Our results confirmed that when the SD_{PEG} was 0.592 PEG/nm^2, corresponding to a D of 1.30 nm, it was enough for the O_H-NLC to maintain its resistance to complement and other plasma proteins, and have a prolonged circulation time.

Both our study[14] and Zhang's[15] have revealed that the long-circulation effect in vivo of PEGylated liposomes was affected after octreotide modification. There was no effect on the pharmacokinetics behavior for OPMS modified NLCs. Moreover, OPMS modified NLCs have superior stealth effects compared with PGMS modified NLCs at the same amounts of modified materials used. It was possible that the hydrophilic PEG chains might insert into aqueous interior of liposomes which would interfere the integrity of phospholipid bilayers, reduce the stability and accelerate the drug leakage. For NLCs, the matrix structure of hydrophobic core would be more stable and the inserting PEG chains could not affect the matrix integrity.

Cellular Uptake of NLCs. Research on nanoparticles labeled with fluorescent dyes was frequently used to study cellular uptake in vitro. Figure 6 shows the qualitative observation of cellular uptake study by fluorescence microscopy. In SMMC-7721 the fluorescent intensity of different preparations was basically in the following order: O_H-NLC > O_L-NLC > NLC > P_L-NLC > P_H-NLC (Figure 6 a(A−E)), however, in L02 the order of fluorescent intensity was O_H-NLC ≈ O_L-NLC ≈ NLC > P_L-NLC > P_H-NLC (Figure 6 b(A−E)). The fluorescence intensity of PGMS modified NLCs in Figure 6 A−C was weaker than NLC both in SMMC-7721 and in L02. The decreased uptake of stealth fluorescent NLC might be dependent on the presence of the PEG chains on the surface of NLC, which formed a hydrophilic cloud.[64,65] As the percentage of the stealth agent added increased, the decreased effect was enhanced, which meant that the excessive hydrophilicity acted as a barrier to prevent NLCs from approaching the cell membrane. Meanwhile, for NLC, P_L-NLC and P_H-NLC, the zeta potential was −19.2 ± 1.1, −7.4 ± 0.87 and −4.5 ± 1.4 mV respectively. The electronic repulsion between NLC and SMMC-7721 or L02 resulted in fewer nanoparticles being adsorbed to SMMC-7721 or L02 compared with P_L-NLC and P_H-NLC. But in this experiment surface hydrophobic/hydrophilic balance of NLC was considered to be the key character to determine the cellular uptake efficiency.

Interestingly, as shown in Figure 6A,D,E, two cell lines almost had the same fluorescent intensity in Figure 6A, but the uptake of the O_L-NLC and O_H-NLC by SMMC-7721 significantly enhanced on contrast with that of L02. Because of overexpessing SSTRs by SMMC-7721 the targeting moiety of octreotide modified on the surface of NLC showed the tumor-targeting property significantly, suggesting that the mechanism of uptake of O_L-NLC and O_H-NLC in SMMC-7721 could be somatostatin receptor mediated endocytosis. The more OPMS incorporated, the stronger the fluorescence intensity was. So we concluded that somatostatin receptor mediated endocytosis was OPMS concentration-dependent and not influenced by the hydrophilicity and stereospecific blockade of PEG chains. The in vitro properties of octreotide mediated uptake were coincident with the in vivo results of tissue distribution, where O_H-NLC remarkably

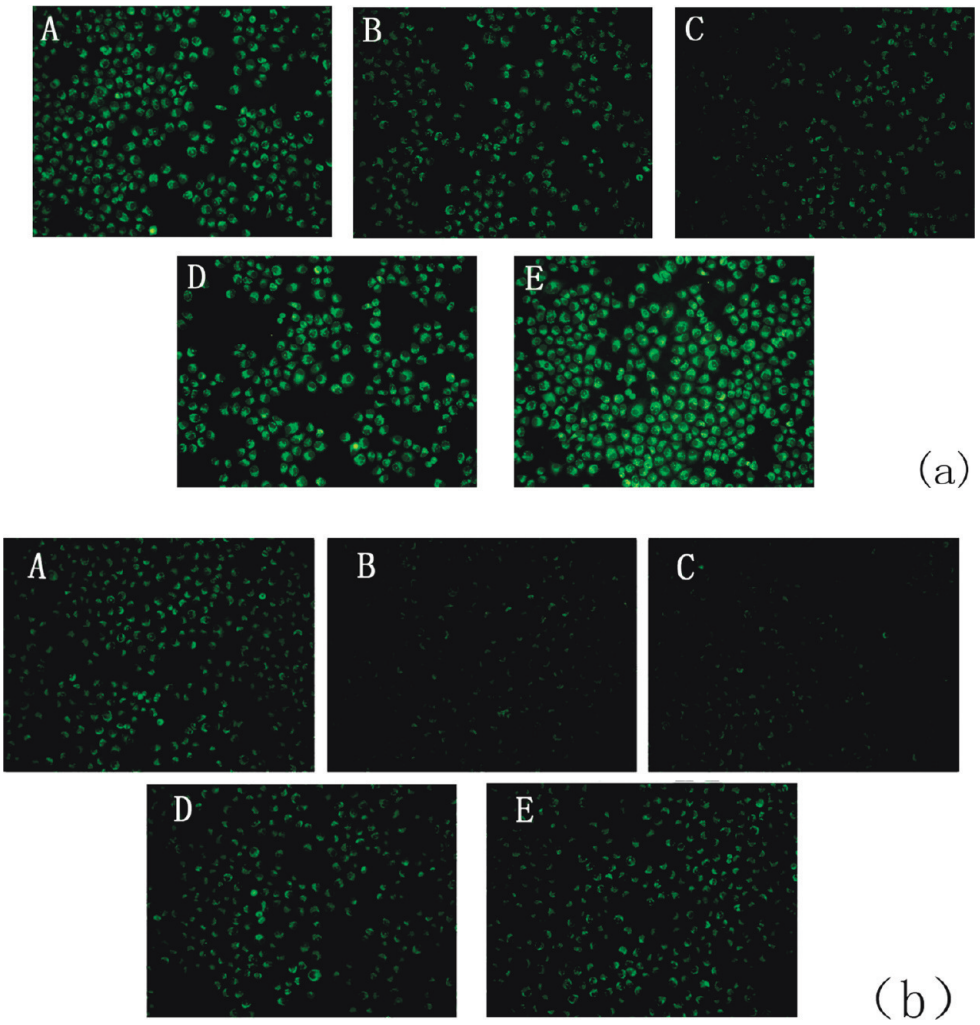

Figure 6. The fluorescent microscopy images of SMMC-7721 (a) and L02 (b) cells after incubation with (A) NLC, (B) P_L-NLC, (C) P_H-NLC, (D) O_L-NLC, (E) O_H-NLC with 500 ng/mL of coumarin-6 at 37 °C for 2 h.

increased the accumulation of HCPT in tumors in S180 tumor-bearing mice, where the area under the concentration−time curves (AUC) of HPCT in the tumor for O_H-NLC was 1.95, 4.25, and 11.05 times more than that of P_H-NLC, NLC and HCPT-injection, respectively.

Conclusion. A novel octreotide−PEG-lipid conjugate has been synthesized and characterized within this study. The NLC loading HCPT modified by two different amounts of PGMS with passive targeting property and OPMS with active targeting property were evaluated. The modified NLCs showed sustained release effect, plasma stability and long-circulating effect. In addition, with increasing the amount of PGMS and OPMS all of the effects mentioned above enhanced and exhibited modification content-dependent. Moreover, the tumor cell uptake for OPMS modified NLCs was significantly higher than that for NLC and PGMS modified NLCs because of the recognition of SSTRs. All data showed that OPMS modified NLC had excellent targeting properties in vitro and in vivo. The higher modification level would enhance the targeting delivery effect. Both the unmodified NLC and modified NLCs without loading HCPT have no cytotoxic impacts in SMMC-7721 and L02 cell lines using MTT assays. All the NLC preparations were safe on two kinds of cells, even at the highest concentration (2 mg/mL), the cell viability was over 90% for 24 h. At the same time the hemolysis assay indicated that even at the highest particle concentration (5 mg/mL) of NLCs, the relative hemolytic activity was lower than 3%. Therefore, the design of the active targeting NLC as nanocarriers by modifying OPMS could be one of the practicable methods to delivery chemotherapeutics to tumor. Further studies should be carried out on the antitumor effects in vitro and in vivo and the mechanism of intracellular uptake.

■ ASSOCIATED CONTENT

Supporting Information. Tables of AIC values for in vitro release of HCPT-loaded NLCs in PBS7.4, PBS6.5, and PBS5.4, table of IC_{50} values of HCPT injection and HCPT-loaded NLCs against SMMC-7721 and L02 cell lines, and additional experimental details. This material is available free of charge via the Internet at http://pubs.acs.org.

■ AUTHOR INFORMATION

Corresponding Author

*State Key Laboratory of Natural Medicines, China Pharmaceutical University, 24 Tong Jia Xiang, Nanjing, 210009 China.

Tel: 1-86-25-83271092. Fax: 1-86-25-83301606. E-mail: pingqn@cpu.edu.cn.

■ ACKNOWLEDGMENT

This work was supported by the project of the National Natural Science Foundation of China (30873183), the major project of the National Science and Technology of China, for new drug development (2009ZX09310-004 and 2009ZX09503-028), the Fundamental Research Funds for the Central Universities (JKQ2009018), and Natural Science Foundation of Jiangsu province (SBK200922895).

■ REFERENCES

(1) Su, J. C.; Tseng, C. L.; Chang, T. G.; Yu, W. J.; Wu, S. K. A synthetic method for peptide-PEG-lipid conjugates: application of octreotide-PEG-DSPE synthesis. *Bioorg. Med. Chem. Lett.* **2008**, *18* (16), 4593–4596.

(2) Lukyanov, A. N.; Elbayoumi, T. A.; Chakilam, A. R.; Torchilin, V. P. Tumor-targeted liposomes: doxorubicin-loaded long-circulating liposomes modified with anti-cancer antibody. *J. Controlled Release* **2004**, *100* (1), 135–144.

(3) Torchilin, V. P.; Rammohan, R.; Weissig, V.; Levchenko, T. S. TAT peptide on the surface of liposomes affords their efficient intracellular delivery even at low temperature and in the presence of metabolic inhibitors. *Proc. Natl. Acad. Sci. U.S.A.* **2001**, *98* (15), 8786–8791.

(4) Lamberts, S. W.; de Herder, W. W.; Hofland, L. J. Somatostatin analogs in the diagnosis and treatment of cancer. *Trends Endocrinol. Metab.* **2002**, *13* (10), 451–457.

(5) Reubi, J. C. Peptide receptors as molecular targets for cancer diagnosis and therapy. *Endocr. Rev.* **2003**, *24* (4), 389–427.

(6) Reubi, J. C. Somatostatin and other Peptide receptors as tools for tumor diagnosis and treatment. *Neuroendocrinology* **2004**, *80* (Suppl. 1), 51–56.

(7) Siehler, S.; Seuwen, K.; Hoyer, D. [125I][Tyr3]octreotide labels human somatostatin sst2 and sst5 receptors. *Eur. J. Pharmacol.* **1998**, *348* (2−3), 311–320.

(8) Krenning, E. P.; Kwekkeboom, D. J.; Bakker, W. H.; Breeman, W. A.; Kooij, P. P.; Oei, H. Y.; van Hagen, M.; Postema, P. T.; de Jong, M.; Reubi, J. C.; et al. Somatostatin receptor scintigraphy with [111In-DTPA-D-Phe1]- and [123I-Tyr3]-octreotide: the Rotterdam experience with more than 1000 patients. *Eur. J. Nucl. Med.* **1993**, *20* (8), 716–731.

(9) Bodei, L.; Cremonesi, M.; Zoboli, S.; Grana, C.; Bartolomei, M.; Rocca, P.; Caracciolo, M.; Macke, H. R.; Chinol, M.; Paganelli, G. Receptor-mediated radionuclide therapy with 90Y-DOTATOC in association with amino acid infusion: a phase I study. *Eur. J. Nucl. Med. Mol. Imaging* **2003**, *30* (2), 207–216.

(10) Shen, H.; Hu, D.; Du, J.; Wang, X.; Liu, Y.; Wang, Y.; Wei, J. M.; Ma, D.; Wang, P.; Li, L. Paclitaxel-octreotide conjugates in tumor growth inhibition of A549 human non-small cell lung cancer xenografted into nude mice. *Eur. J. Pharmacol.* **2008**, *601* (1−3), 23–29.

(11) Huang, C. M.; Wu, Y. T.; Chen, S. T. Targeting delivery of paclitaxel into tumor cells via somatostatin receptor endocytosis. *Chem. Biol.* **2000**, *7* (7), 453–461.

(12) Moody, T. W.; Fuselier, J.; Coy, D. H.; Mantey, S.; Pradhan, T.; Nakagawa, T.; Jensen, R. T. Camptothecin-somatostatin conjugates inhibit the growth of small cell lung cancer cells. *Peptides* **2005**, *26* (9), 1560–1566.

(13) Osapay, G.; Prokai, L.; Kim, H. S.; Medzihradszky, K. F.; Coy, D. H.; Liapakis, G.; Reisine, T.; Melacini, G.; Zhu, Q.; Wang, S. H.; Mattern, R. H.; Goodman, M. Lanthionine-somatostatin analogs: synthesis, characterization, biological activity, and enzymatic stability studies. *J. Med. Chem.* **1997**, *40* (14), 2241–2251.

(14) Sun, M. J.; Wang, Y.; Shen, J.; Xiao, Y. Y.; Su, Z. G.; Ping, Q. N. Octreotide-modification enhances the delivery and targeting of doxorubicin-loaded liposomes to somatostatin receptors expressing tumor in vitro and in vivo. *Nanotechnology* **2010**, *21* (47), 475101.

(15) Zhang, J.; Jin, W.; Wang, X.; Wang, J.; Zhang, X.; Zhang, Q. A novel octreotide modified lipid vesicle improved the anticancer efficacy of doxorubicin in somatostatin receptor 2 positive tumor models. *Mol. Pharmaceutics* **2010**, *7* (4), 1159–1168.

(16) Han, F.; Li, S. M.; Yin, R.; Liu, H. Z.; Xu, L. Effect of surfactants on the formation and characterization of a new type of colloidal drug delivery system: Nanostructured lipid carriers. *Colloids Surf., A* **2008**, *315* (1−3), 210–216.

(17) Doktorovova, S.; Araujo, J.; Garcia, M. L.; Rakovsky, E.; Souto, E. B. Formulating fluticasone propionate in novel PEG-containing nanostructured lipid carriers (PEG-NLC). *Colloids Surf., B* **2010**, *75* (2), 538–542.

(18) Bondi, M. L.; Craparo, E. F.; Giammona, G.; Cervello, M.; Azzolina, A.; Diana, P.; Martorana, A.; Cirrincione, G. Nanostructured lipid carriers-containing anticancer compounds: Preparation, characterization, and cytotoxicity studies. *Drug Delivery* **2007**, *14* (2), 61–67.

(19) Utreja, S.; Khopade, A. J.; Jain, N. K. Lipoprotein-mimicking biovectorized systems for methotrexate delivery. *Pharm. Acta Helv.* **1999**, *73* (6), 275–279.

(20) Joshi, M. D.; Muller, R. H. Lipid nanoparticles for parenteral delivery of actives. *Eur. J. Pharm. Biopharm.* **2009**, *71* (2), 161–172.

(21) Garcia-Fuentes, M.; Torres, D.; Martin-Pastor, M.; Alonso, M. J. Application of NMR spectroscopy to the characterization of PEG-stabilized lipid nanoparticles. *Langmuir* **2004**, *20* (20), 8839–8845.

(22) Wan, F.; You, J.; Sun, Y.; Zhang, X. G.; Cui, F. D.; Du, Y. Z.; Yuan, H.; Hu, F. Q. Studies on PEG-modified SLNs loading vinorelbine bitartrate (I): preparation and evaluation in vitro. *Int. J. Pharm.* **2008**, *359* (1−2), 104–110.

(23) Li, Y. F.; Zhang, R. Reversed-phase high-performance liquid chromatography method for the simultaneous quantitation of the lactone and carboxylate forms of the novel natural product anticancer agent 10-hydroxycamptothecin in biological fluids and tissues. *J. Chromatogr., B: Biomed. Sci. Appl.* **1996**, *686* (2), 257–265.

(24) Nicholas, A. R.; Scott, M. J.; Kennedy, N. I.; Jones, M. N. Effect of grafted polyethylene glycol (PEG) on the size, encapsulation efficiency and permeability of vesicles. *Biochim. Biophys. Acta* **2000**, *1463* (1), 167–178.

(25) Li, S. D.; Huang, L. Nanoparticles evading the reticuloendothelial system: role of the supported bilayer. *Biochim. Biophys. Acta* **2009**, *1788* (10), 2259–2266.

(26) Shen, J.; Wang, Y.; Ping, Q. N.; Xiao, Y. Y.; Huang, X. Mucoadhesive effect of thiolated PEG stearate and its modified NLC for ocular drug delivery. *J. Controlled Release* **2009**, *137* (3), 217–223.

(27) Ding, F.; Huang, J.; Lin, J.; Li, Z.; Liu, F.; Jiang, Z.; Sun, Y. A study of the binding of C.I. Mordant Red 3 with bovine serum albumin using fluorescence spectroscopy. *Dyes Pigm.* **2009**, *82* (1), 65–70.

(28) Nikanjam, M.; Gibbs, A. R.; Hunt, C. A.; Budinger, T. F.; Forte, T. M. Synthetic nano-LDL with paclitaxel oleate as a targeted drug delivery vehicle for glioblastoma multiforme. *J. Controlled Release* **2007**, *124* (3), 163–171.

(29) Lu, B.; Xiong, S. B.; Yang, H.; Yin, X. D.; Chao, R. B. Solid lipid nanoparticles of mitoxantrone for local injection against breast cancer and its lymph node metastases. *Eur. J. Pharm. Sci.* **2006**, *28* (1−2), 86–95.

(30) Sadzuka, Y.; Nakade, A.; Hirama, R.; Miyagishima, A.; Nozawa, Y.; Hirota, S.; Sonobe, T. Effects of mixed polyethyleneglycol modification on fixed aqueous layer thickness and antitumor activity of doxorubicin containing liposome. *Int. J. Pharm.* **2002**, *238* (1−2), 171–180.

(31) Peracchia, M. T.; Vauthier, C.; Passirani, C.; Couvreur, P.; Labarre, D. Complement consumption by poly(ethylene glycol) in different conformations chemically coupled to poly(isobutyl 2-cyanoacrylate) nanoparticles. *Life Sci.* **1997**, *61* (7), 749–761.

(32) Torchilin, V. P.; Levchenko, T. S.; Lukyanov, A. N.; Khaw, B. A.; Klibanov, A. L.; Rammohan, R.; Samokhin, G. P.; Whiteman, K. R. p-Nitrophenylcarbonyl-PEG-PE-liposomes: fast and simple attachment of specific ligands, including monoclonal antibodies, to distal ends of

PEG chains via p-nitrophenylcarbonyl groups. *Biochim. Biophys. Acta* **2001**, *1511* (2), 397–411.

(33) Lim, S. J.; Kim, C. K. Formulation parameters determining the physicochemical characteristics of solid lipid nanoparticles loaded with all-trans retinoic acid. *Int. J. Pharm.* **2002**, *243* (1−2), 135–146.

(34) Liang, X.; Mao, G.; Ng, K. Y. Effect of chain lengths of PEO-PPO-PEO on small unilamellar liposome morphology and stability: an AFM investigation. *J. Colloid Interface Sci.* **2005**, *285* (1), 360–372.

(35) McNeeley, K. M.; Annapragada, A.; Bellamkonda, R. V. Decreased circulation time offsets increased efficacy of PEGylated nanocarriers targeting folate receptors of glioma. *Nanotechnology* **2007**, *18* (38), 385101.

(36) Fang, C.; Shi, B.; Pei, Y. Y.; Hong, M. H.; Wu, J.; Chen, H. Z. In vivo tumor targeting of tumor necrosis factor-alpha-loaded stealth nanoparticles: effect of MePEG molecular weight and particle size. *Eur. J. Pharm. Sci.* **2006**, *27* (1), 27–36.

(37) Zimmermann, E.; Muller, R. H. Electrolyte- and pH-stabilities of aqueous solid lipid nanoparticle (SLN) dispersions in artificial gastrointestinal media. *Eur. J. Pharm. Biopharm.* **2001**, *52* (2), 203–210.

(38) Sriamornsak, P.; Thirawong, N.; Nunthanid, J.; Puttipipatkhachorn, S.; Thongborisute, J.; Takeuchi, H. Atomic force microscopy imaging of novel self-assembling pectin-liposome nanocomplexes. *Carbohydr. Polym.* **2008**, *71* (2), 324–329.

(39) Gualbert, J.; Shahgaldian, P.; Coleman, A. W. Interactions of amphiphilic calix[4]arene-based Solid Lipid Nanoparticles with bovine serum albumin. *Int. J. Pharm.* **2003**, *257* (1−2), 69–73.

(40) Shahgaldian, P.; Da Silva, E.; Coleman, A. W.; Rather, B.; Zaworotko, M. J. Para-acyl-calix-arene based solid lipid nanoparticles (SLNs): a detailed study of preparation and stability parameters. *Int. J. Pharm.* **2003**, *253* (1−2), 23–38.

(41) Shimada, K.; Miyagishima, A.; Sadzuka, Y.; Nozawa, Y.; Mochizuki, Y.; Ohshima, H.; Hirota, S. Determination of the thickness of the fixed aqueous layer around polyethyleneglycol-coated liposomes. *J. Drug Targeting* **1995**, *3* (4), 283–289.

(42) Sadzuka, Y.; Sugiyama, I.; Tsuruda, T.; Sonobe, T. Characterization and cytotoxicity of mixed polyethyleneglycol modified liposomes containing doxorubicin. *Int. J. Pharm.* **2006**, *312* (1−2), 83–89.

(43) Shi, B.; Fang, C.; You, M. X.; Hong, M. H.; Pei, Y. Y. Stealth PEG-PHDCA niosomes: effects of chain length of PEG on niosomes in vitro complement consumption and phagocytic uptake. *Yaoxue Xuebao* **2005**, *40* (11), 976–981.

(44) Needham, D.; Stoicheva, N.; Zhelev, D. V. Exchange of monooleoylphosphatidylcholine as monomer and micelle with membranes containing poly(ethylene glycol)-lipid. *Biophys. J.* **1997**, *73* (5), 2615–2629.

(45) Du, H.; Chandaroy, P.; Hui, S. W. Grafted poly-(ethylene glycol) on lipid surfaces inhibits protein adsorption and cell adhesion. *Biochim. Biophys. Acta* **1997**, *1326* (2), 236–248.

(46) Klibanov, A. L.; Maruyama, K.; Beckerleg, A. M.; Torchilin, V. P.; Huang, L. Activity of amphipathic poly(ethylene glycol) 5000 to prolong the circulation time of liposomes depends on the liposome size and is unfavorable for immunoliposome binding to target. *Biochim. Biophys. Acta* **1991**, *1062* (2), 142–148.

(47) Kenworthy, A. K.; Hristova, K.; Needham, D.; McIntosh, T. J. Range and magnitude of the steric pressure between bilayers containing phospholipids with covalently attached poly(ethylene glycol). *Biophys. J.* **1995**, *68* (5), 1921–1936.

(48) Owens, D. E., 3rd; Peppas, N. A. Opsonization, biodistribution, and pharmacokinetics of polymeric nanoparticles. *Int. J. Pharm.* **2006**, *307* (1), 93–102.

(49) Shimada, K.; Matsuo, S.; Sadzuka, Y.; Miyagishima, A.; Nozawa, Y.; Hirota, S.; Sonobe, T. Determination of incorporated amounts of poly(ethylene glycol)-derivatized lipids in liposomes for the physicochemical characterization of stealth liposomes. *Int. J. Pharm.* **2000**, *203* (1−2), 255–263.

(50) Torchilin, V. P.; Omelyanenko, V. G.; Papisov, M. I.; Bogdanov, A. A., Jr.; Trubetskoy, V. S.; Herron, J. N.; Gentry, C. A. Poly(ethylene glycol) on the liposome surface: on the mechanism of polymer-coated liposome longevity. *Biochim. Biophys. Acta* **1994**, *1195* (1), 11–20.

(51) Rex, S.; Zuckermann, M. J.; Lafleur, M.; Silvius, J. R. Experimental and Monte Carlo simulation studies of the thermodynamics of polyethyleneglycol chains grafted to lipid bilayers. *Biophys. J.* **1998**, *75* (6), 2900–2914.

(52) Soong, R.; Macdonald, P. M. PEG molecular weight and lateral diffusion of PEG-ylated lipids in magnetically aligned bicelles. *Biochim. Biophys. Acta* **2007**, *1768* (7), 1805–1814.

(53) Gref, R.; Domb, A.; Quellec, P.; Blunk, T.; Muller, R. H.; Verbavatz, J. M.; Langer, R. The Controlled Intravenous Delivery of Drugs Using Peg-Coated Sterically Stabilized Nanospheres. *Adv. Drug Delivery Rev.* **1995**, *16* (2−3), 215–233.

(54) Large, V.; Arner, P.; Reynisdottir, S.; Grober, J.; Van Harmelen, V.; Holm, C.; Langin, D. Hormone-sensitive lipase expression and activity in relation to lipolysis in human fat cells. *J. Lipid Res.* **1998**, *39* (8), 1688–1695.

(55) Ruge, T.; Sukonina, V.; Myrnas, T.; Lundgren, M.; Eriksson, J. W.; Olivecrona, G. Lipoprotein lipase activity/mass ratio is higher in omental than in subcutaneous adipose tissue. *Eur. J. Clin. Invest.* **2006**, *36* (1), 16–21.

(56) Kobayashi, J.; Kusunoki, M.; Murase, Y.; Kawashiri, M.; Higashikata, T.; Miwa, K.; Katsuda, S.; Takata, M.; Asano, A.; Nohara, A.; Inazu, A.; Mabuchi, H. Relationship of lipoprotein lipase and hepatic triacylglycerol lipase activity to serum adiponectin levels in Japanese hyperlipidemic men. *Horm. Metab. Res.* **2005**, *37* (8), 505–509.

(57) Derakhshandeh, K.; Erfan, M.; Dadashzadeh, S. Encapsulation of 9-nitrocamptothecin, a novel anticancer drug, in biodegradable nanoparticles: factorial design, characterization and release kinetics. *Eur. J. Pharm. Biopharm.* **2007**, *66* (1), 34–41.

(58) Costa, P.; Sousa Lobo, J. M. Modeling and comparison of dissolution profiles. *Eur. J. Pharm. Sci.* **2001**, *13* (2), 123–133.

(59) Barzegar-Jalali, M.; Adibkia, K.; Valizadeh, H.; Shadbad, M. R.; Nokhodchi, A.; Omidi, Y.; Mohammadi, G.; Nezhadi, S. H.; Hasan, M. Kinetic analysis of drug release from nanoparticles. *J. Pharm. Pharm. Sci.* **2008**, *11* (1), 167–177.

(60) Morales, M. E.; Gallardo Lara, V.; Calpena, A. C.; Domenech, J.; Ruiz, M. A. Comparative study of morphine diffusion from sustained release polymeric suspensions. *J. Controlled Release* **2004**, *95* (1), 75–81.

(61) Goppert, T. M.; Muller, R. H. Adsorption kinetics of plasma proteins on solid lipid nanoparticles for drug targeting. *Int. J. Pharm.* **2005**, *302* (1−2), 172–186.

(62) Harnisch, S.; Muller, R. H. Adsorption kinetics of plasma proteins on oil-in-water emulsions for parenteral nutrition. *Eur. J. Pharm. Biopharm.* **2000**, *49* (1), 41–46.

(63) Aggarwal, P.; Hall, J. B.; McLeland, C. B.; Dobrovolskaia, M. A.; McNeil, S. E. Nanoparticle interaction with plasma proteins as it relates to particle biodistribution, biocompatibility and therapeutic efficacy. *Adv. Drug Delivery Rev.* **2009**, *61* (6), 428–437.

(64) Hu, Y.; Xie, J.; Tong, Y. W.; Wang, C. H. Effect of PEG conformation and particle size on the cellular uptake efficiency of nanoparticles with the HepG2 cells. *J. Controlled Release* **2007**, *118* (1), 7–17.

(65) Abu Lila, A. S.; Kizuki, S.; Doi, Y.; Suzuki, T.; Ishida, T.; Kiwada, H. Oxaliplatin encapsulated in PEG-coated cationic liposomes induces significant tumor growth suppression via a dual-targeting approach in a murine solid tumor model. *J. Controlled Release* **2009**, *137* (1), 8–14.